Charging effects and bistability in resonant quantum wire structures

1994 J. Phys.: Condens. Matter 6 5507

(http://iopscience.iop.org/0953-8984/6/28/023)

J. Phys.: Condens. Matter 6 (1994) 5507–5519. Printed in the UK

Charging effects and bistability in resonant quantum wire structures

Igor Zozulenko†
Division of Physics, The Norwegian Institute of Technology, N-7034, Trondheim, Norway

Received 2 February 1994, in final form 22 April 1994

Abstract. Ballistic electron transport in resonant quantum-wire structures (double point contacts in series) is investigated taking into account charge build-up effects. It is shown that when the resonant condition holds (i.e. when the Fermi energy of incoming electrons coincides with the energy of the quasibound state), the charge stored in the structure may lead to a bistable behaviour of the system. In the linear-response approximation, when the current flowing through the structure is described by the two-terminal Landauer formula, a closed non-linear equation is derived relating the transmitted current to the energy of the resonant level and the width of the resonance Γ. It is shown that the condition that must be satisfied for bistability to occur is $e^3V/\pi C\Gamma^2 \gtrsim 1$, where V is the applied bias and C is the capacitance of the structure. The dependence of the width of the resonant level and its position on the device geometry is investigated using the match-mode technique for calculations of the electron transmission coefficient. The width of the resonance is shown to increase with increasing length of the contacts, but the position of the resonant level (in units of the propagation threshold energy in the contact regions) is insensitive to the length of the contacts as well as to the lengths of the side arms. On the basis of the results obtained, the bistability in the I–V_g characteristic (current–gate voltage) is studied for structures of realistic dimensions.

1. Introduction

Following advances in fabrication and improvement of vertical double-barrier resonant tunnelling (DBRT) semiconductor structures, where electrons move in the direction perpendicular to the plane of confinement, the new generation of nanometre lateral structures has emerged, where a two-dimensional electron gas (2DEG) defined on the top of a heterostructure can be further confined to one or zero dimension by means of a split-gate technique (see, for example, [1]). Modern submicrometre lithographic technology makes it possible to fabricate structures with dimensions smaller than the electron phase coherence length, where the electron transport is fully ballistic. In this case electrons propagate coherently over the entire device like light through a waveguide and the device conductance is determined by the potential induced in the 2DEG by the split gate. When the Fermi wavelength of electrons λ_F is of the order of the width of the structure (typical values of λ_F currently achieved in real GaAs–AlGaAs structures lie in the range of 100–30 nm [2]), the confinement in the direction perpendicular to the electron motion causes a variety of novel effects. Among them we mention only the following two: the quantized conductance of a quantum point contact (QPC) resulting from changes in the number of 1D subbands contributing to the current [3], and the existence of quasibound states below

† On leave of absence from the Bogolyubov Institute for Theoretical Physics, Academy of Sciences of the Ukraine, Kiev, 252143, Ukraine.

0953-8984/94/285507+13$19.50

the propagation threshold at the intersection of quantum wires which are unable to trap classical particles [4]. These effects are exploited in a resonant quantum-wire structure (RQWS) consisting of two narrow constrictions (QPCs) defined in the wide wire [5–7], or in the 2DEG [8], see figure 1. Weishaar *et al* [6] have predicted that this device may exhibit a negative differential resistance up to approximately 60 K with a peak-to-valley ratio of over 80:1 at zero temperature. The operation of the device is quite similar to that of the double-barrier resonant tunnelling diode. Indeed, when the Fermi energy E_F of incoming electrons in the left wide wire (emitter) is less than the propagation threshold in the narrow constriction, E^{th}, there are no propagating modes in the narrow constriction, and the total transmission is nearly zero. But when the Fermi energy, still below E^{th}, is tuned to the energy of the bound state which resides in the cavity, resonant transport to the right wide wire (collector) based on evanescent mode coupling occurs.

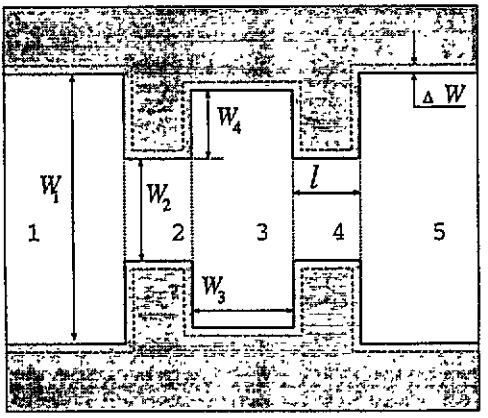

Figure 1. Schematic view of the resonant quantum waveguide structure. Regions 1 and 5 are the emitter and collector wires; regions 2 and 4 are the narrow wires (constrictions); region 3 is the cavity. Dashed lines represent the changes of the device geometry due to the varying of the gate voltage.

Many important features of electron transport in submicrometre structures are associated with non-linear phenomena caused by the space–charge formation inside the structure. The above phenomena have been extensively studied in vertical structures, both theoretically [9–16], and experimentally [17]. It has been demonstrated that the charge build-up in the well of DBRT structures may shift the resonance energy and the potential distribution through the system and eventually may lead to bistability and hysteresis in the I–V characteristic. The origin of the two different states in the I–V characteristic stems from the difference in the ways by which one can align the Fermi sea in the emitter and the resonant level in the well of the DBRT structure. More precisely, if the resonant level approaches the Fermi energy from above (by increasing the bias voltage), negative electrostatic feedback occurs, since the lowering of the resonant level is compensated by its upward shift due to the charge build-up in the well. As a result, resonant transmission occurs at a bias higher than that in the case when no space–charge formation is taken into account. In contrast, if the resonant level approaches the bottom of the conduction band from below, positive electrostatic feedback takes place. Therefore, two different values of the transmitted current correspond to the same external bias, depending on whether one reaches resonant transmission by increasing

the bias voltage (from the state with a filled well) or by decreasing it (from the state with an empty well).

A number of experimental [18, 19] and theoretical [20, 21] studies deal with charging effects in lateral semiconductor structures. In particular, in quantum-dot structures 'Coulomb blockade' effects [22] manifest themselves in the so-called Coulomb oscillations in the conductance and in the Coulomb staircase in the I–V characteristic of quantum-dot structures. On the other hand, the spectral and transport properties of RQWSs have until now been studied only in the linear regime, where effects of the space–charge formation have not been taken into account. The main aim of the present study is to investigate the charging effects in the RQWS and its influence on the device conductance.

The paper is organized as follows. In section 2 resonant transmission of electrons in RQWSs is studied taking into account the charging of the structure. The current flowing through the device is related to the characteristics of the structure: the energy of the quasibound level and the escape rate of the electron from the quasibound state. These characteristics are calculated in section 3 on the basis of a match-mode technique. The results obtained in sections 2 and 3 are used in section 4 for the calculation of the current–gate voltage characteristic of an RQWS of realistic dimensionality. A brief summary of the work is given in section 5.

2. Effects of the space–charge formation on resonant electron transport

In the limit of sufficiently low temperatures in the linear-response regime, when incoming and outgoing electrons are characterized by the equilibrium Fermi distribution and their electrochemical potentials, $\mu_{l(r)}$, deviate only slightly, the current flowing through the 2D lateral structure is given by the two-terminal Landauer formula [23], and is determined by the total transmission $T(E)$ evaluated at the Fermi energy E_F

$$I = \frac{2e^2}{h} T(E_F) V \tag{1}$$

where $V = (\mu_l - \mu_r)/e$ is the voltage drop across the device. As was mentioned in the introduction, operation of the RQWS exploits the resonance transport regime, thus, in this section we shall focus on the electron transmission through the quasibound state.

For energies close to that of the quasibound state the transmission probability is Lorenzian and given by the Breit–Wigner formula [24]

$$T(E) = \frac{4\Gamma_l\Gamma_r/\Gamma^2}{1 + ((E - E_r)/(\Gamma/2))^2} \tag{2}$$

where E is the energy of the incident electrons and E_r is the energy of the quasibound state (both are measured from the bottom of the conduction band of the emitter), $\Gamma_{l(r)}/\hbar$ is the escape rate of electrons from the quasibound state to the left (right) reservoir, and $\Gamma = \Gamma_l + \Gamma_r$ is the total width of the transmission peak. Note that equation (2) is valid when the difference $E - E_r$ is small in comparison to the distance to the nearest quasibound state or to the region of the continuous spectrum, and the use of the Landauer formula for the description of resonant transmission is justified when the imbalance of chemical potentials of right and left reservoirs is small in comparison with the characteristic changes of transmission coefficients, i.e. $eV \ll \Gamma$ [25].

When charging effects are disregarded, the energy of the quasibound state $E_r = E_r^0$ is determined by the device geometry (calculation of E_r^0 and Γ is the subject of the next section). In the vicinity of the resonance, the charge stored inside the device increases by several orders of magnitude in comparison with its off-resonant value (see below), thereby shifting the bottom of the conduction band in the cavity. To take into account the charging effects, we shall follow Sheard and Toombs [10] who used simple electrostatic considerations in their treatment of the bistability effects in the vertical DBRT structures. Thus, the shift of the conduction band in the cavity due to the excess charge Q is taken to be equal to the electrostatic energy associated with the charging of the structure

$$\Delta E = \frac{eQ}{C} \tag{3}$$

where C is the capacitance of the cavity (region 3 in figure 1). The energy of the quasibound level is then

$$E_r = E_r^0 + \frac{eQ}{C} \tag{4}$$

where we have dropped the term $-\frac{1}{2}eV$ that describes the shift of the bottom of the conduction band in the cavity due to the applied voltage, since $eV \ll E_r^0$ in the linear-response regime considered here. One can show that this approach is equivalent to the Hartree approximation used by Davydov and Ermakov [9] for the description of the space–charge formation in the DBRT structures.

The charge Q stored in the dot is related to the current flowing through the structure by $I = (\Gamma_r/\hbar)Q$. Hereafter we shall restrict ourselves to the case of a symmetrical structure when under resonance conditions, $E = E_r$, full transmission, $T = 1$, is achieved and, therefore, charging effects are most pronounced. In this case, $\Gamma_l = \Gamma_r = \Gamma/2$ and the excess charge appears in the form

$$Q = \frac{2\hbar}{\Gamma} I. \tag{5}$$

Combining (1)–(5) we find a closed non-linear equation for $y = I/I_{max}$

$$y(\varepsilon) = \frac{1}{1 + (\varepsilon - \alpha y(\varepsilon))^2} \tag{6}$$

where $I_{max} = 2e^2V/h$ is the resonant current, $\varepsilon = (E - E_r^0)/(\Gamma/2)$ and $\alpha = 4e^3V/(C\pi\Gamma^2)$.

Note that a similar cubic equation for the transmission coefficient has been obtained by Davydov and Ermakov [9] for the case of non-linear resonant tunnelling of high-density electrons through a system of two identical barriers, and by Malysheva and Onipko [15] who used the tight-binding Hamiltonian including the Hubbard electron–electron interaction to study an electron tunnelling through a single guest molecule in a 1D molecular chain.

Simple analysis shows that equation (6) has three roots when $\alpha \gtrsim \frac{3}{2}$. This condition determines the region of bistable behaviour of the system which, with regards to equation (3), can be rewritten in the form

$$\frac{\Delta E_{max}}{\Gamma/2} \gtrsim \frac{3}{2} \tag{7}$$

where $\Delta E_{max} = eQ_{max}/C$, $Q_{max} = 2e^2V/(\pi\Gamma)$. In other words, the maximum shift of the resonant level, ΔE_{max}, caused by the excess charge stored in the cavity must exceed roughly the width of the resonance. If the condition (7) holds, the energy region where one can expect bistability behaviour is

$$E - E_r^0 \sim \frac{eQ_{max}}{C}. \tag{8}$$

Conditions similar to (7) and (8) for the case of 3D electron transport in DBRT structures were obtained for the first time by Rahman and Davies [14], and Sheard and Toombs [10].

Note that in our estimate of the charging energy we neglected the exchange interaction, which, in contrast to the direct Coulomb interaction, lowers the conduction band in the cavity [11, 16]. For the case of DBRT structures the contribution from this interaction is shown [16] to be comparable with that from direct Coulomb interaction only when the maximum electron density in the well is relatively low, $\sim 10^{15}$ m^{-2}. For higher densities (considered here, see below) the exchange electron correlation is unimportant for the conduction band renormalization.

3. Escape rate of electrons and energy level of quasibound state

In the preceding section it has been shown that the current flowing through the RQWS near resonance with charging effects accounted for, is determined (at fixed Fermi energy and applied bias) by the energy of the quasibound level E_r^0 and the escape rate of electrons from the quasibound level $2\Gamma/\hbar$, see equation (6). In this section we shall calculate these two parameters and study their dependence on the geometry of the structure.

We shall use an idealized waveguide model, assuming the split gate to produce a hard-wall confinement and electron transport through the device to be fully ballistic. Then a solution of the time-independent Schrödinger equation in each uniform waveguide section ψ_n, $n = 1, \ldots, 5$ (see figure 1), is given as a complete set of the orthonormal square-well eigenfunctions (transverse modes). Consider incoming electrons with the energy $E_F = \hbar^2 k_F^2/2m^*$ propagating in the pth mode in the emitter lead. The wave functions in the outer regions 1 and 5 can be written in the form

$$\begin{aligned}
\psi_1 &= \sqrt{\frac{2}{w_1}} \sum_j (\delta_{j,p} e^{ik_j^1(x+l+(w_3/2))} + r_j^p e^{-ik_j^1(x+l+(w_3/2))}) \sin\frac{\pi j(y+(w_1/2))}{w_1} \\
\psi_5 &= \sqrt{\frac{2}{w_1}} \sum_j t_j^p e^{-ik_j^1(x-l-(w_3/2))} \sin\frac{\pi j(y+(w_1/2))}{w_1}
\end{aligned} \tag{9}$$

where $k_j^n = (\pi/w_n)\sqrt{(k_F w_n/\pi)^2 - j^2}$ is the longitudinal wave vector of the electron in the jth mode in each region $n = 1, \ldots, 5$ and w_n is the corresponding waveguide width; r_j^p and t_j^p are the reflection and transmission amplitudes. Similar expressions for ψ_n can be written down for regions 2–4. The integer part of the dimensionless wave vector $k_F w_n/\pi$ determines the number of propagating modes in each uniform waveguide section, since k_j^n corresponds to the propagation modes if $k_F w_n/\pi > j$ and the evanescent ones otherwise.

Matching the wave functions and their derivatives on the boundaries of the regions 1–5 using a standard match-mode technique, we obtain for the transmission and reflection amplitudes

$$\overline{r_m} \mp t_m = -\sum_{m'} C_{mm'} \alpha_{m'}^{[\pm]}, \qquad \overline{r_m} = r_m + \delta_{m,p} \tag{10}$$

where $\alpha_j^{[\pm]}$ represent the solution of the infinite set of equations (indexes i and j enumerate modes in the constrictions)

$$\sum_j \alpha_j^{[\pm]} G_{ij} = F_i \qquad i, j = 1, 2, \ldots \tag{11}$$

and

$$G_{ij} = \left[\delta_{i,j}(-f_i^{[\pm]} \coth \kappa_i l [\pm] \sec^2 \kappa_i l) + f_i^{[\pm]} D_{ij} + \delta_{j,\{\substack{e\\o}\}} \coth \kappa_i l \sum_{n\ [\substack{e\\o}]} a_n^{[\pm]} A_{in} A_{nj} \right.$$
$$\left. - \sum_{n\ [\substack{e\\o}]} a_n^{[\pm]} A_{in} \sum_{m\ \{\substack{e\\o}\}} \frac{\sinh \kappa_m l}{\sinh \kappa_i l} A_{nm} D_{mj} \right]$$

$$F_i = -f_i^{[\pm]} B_i(p) + \sum_{n\ [\substack{e\\o}]} a_n^{[\pm]} A_{in} \sum_{m\ \{\substack{e\\o}\}} \frac{\sinh \kappa_m l}{\sinh \kappa_i l} A_{nm} B_m(p)$$

$$A_{mm'} = \frac{2\pi m'}{\kappa_m w_2^2 \sinh \kappa_m w_2} \int_0^{w_2} \mathrm{d}y \, \sin \frac{\pi m y}{w_2} \sinh \frac{\kappa_{m'} y}{w_2}$$

$$B_m(p) = \frac{2\mathrm{i}k_p^1}{\kappa_m} C_{p,m} \qquad \kappa_m = \mathrm{i}k_m^2$$

$$C_{mm'} = \frac{2}{\sqrt{w_1 w_2}} \int_0^{w_2} \mathrm{d}y \, \sin \frac{\pi m y}{w_2} \sin \frac{\pi m'(y + (w_1/2) - (w_2/2))}{w_1}$$

$$D_{mm'} = \frac{1}{\kappa_m} \sum_l \mathrm{i}k_l^1 C_{lm} C_{lm'}$$

$$a_m^{\pm} = \frac{4 \sinh \kappa_m w_4 \sinh \kappa_m w_2}{\sinh \kappa_m w_4 \pm \sinh \kappa_m (w_2 + w_4)} \qquad f_m^{\pm} = \frac{\sinh \kappa_m l \pm \sinh \kappa_m (l + w_2)}{\sinh \kappa_m l \sinh \kappa_m w_2}.$$

The symbols e (even) and o (odd) correspond to the summation over even and odd modes; when i is even (odd) the upper (lower) value in the curly brackets must be taken.

Note that analogous equations can be obtained in the tight-binding approach making use of the Green function techniques, as was demonstrated previously by Onipko *et al* [26] for different waveguide structures.

It is worth stressing that the off-diagonal elements of the matrix G_{ij} are comparable in magnitude with the diagonal ones. This means that strong mode mixing inside the structure occurs. This is in contrast to the case of a single constriction where the diagonal elements of the corresponding matrix are dominant and, therefore, mode mixing is weak.

The transmission probability of the electron entering the device in the pth mode in the emitter is given by

$$T_p = \sum_{m\ (\text{propag})} t_m^p (t_m^p)^* \frac{k_m^1}{k_p^1} \tag{12}$$

where summation runs over only upon propagating modes in the collector region (evanescent modes do not contribute to the current), the maximum propagating mode being determined by the integer part of the value $k_F w_1/\pi$. The total transmission through the device

$$T(E) = \sum_{p\ (\text{propag})} T_p \tag{13}$$

is determined by the contributions from all propagating modes available at the energy E of incoming electrons in the emitter region.

We solve equations (10) and (11) numerically, truncating them at a finite number of modes, N. Calculations show that inclusion of only $N \sim 5$–7 modes in the narrow regions (and, correspondingly, $\sim Nw_1/w_2$ modes in the wide regions) ensures the desired degree of convergence ($< 1\%$) in the energy range of interest. The dependence of the transmission coefficient on the dimensionless wave vector $k \equiv k_F w_2/\pi$ is shown in figure 2. At $k = 1$, when the lowest evanescent mode in the constrictions turns into a propagating one, the transmission exhibits a threshold behaviour, rising from zero to unity. As seen, changing the ratio of widths of the wide and narrow waveguides, w_1/w_2, does not influence the transmission coefficient if $w_1/w_2 \gtrsim 3$. This ratio of widths is taken in all the calculations presented below. We have also calculated the transmission coefficient for the structures considered by Berggren and Ji [8] where emitter and collector regions were the 2DEG, and we found virtually exact agreement.

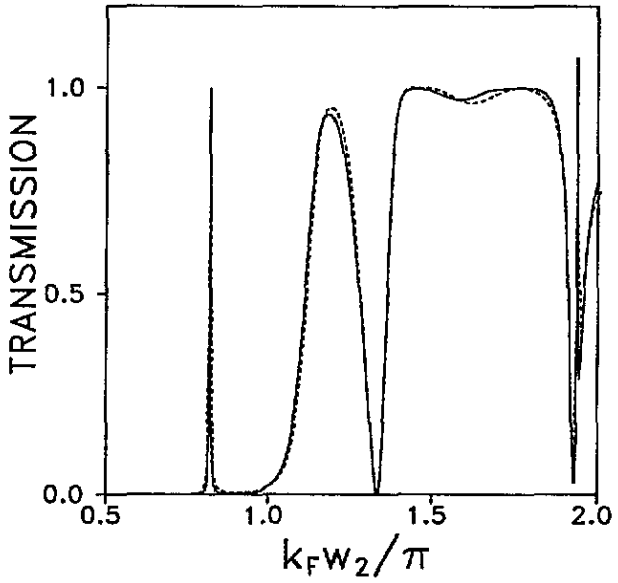

Figure 2. Total transmission as a function of the Fermi wave vector for various ratios $w_1/w_2 = 1.5$ (dashed line), 3, 10 (solid lines; undistinguished in the scale of the figure). The length of the constrictions, the width of the cavity and the length of the sidearms are kept equal to the width of the constrictions, $l = w_3 = w_4 = w_2$.

Two sharp peaks in figure 2 below the propagation threshold for the first ($k = 1$) and the second ($k = 2$) mode in the constrictions correspond to resonant tunnelling through a quasibound state. The dependence of the charge stored in the structure $Q = \int \psi\psi^*$ on the wave vector k (figure 3), showing a sharp peak at the resonant level, also illustrates the existence of a quasibound state in the cavity. In figure 4 a contour plot of the normalized square modulus of the wave function $\psi\psi^*$ is shown for the first resonance ($k \simeq 0.82$). It is seen that the quasibound state resides at the intersection of the wires and does not extend to the side arms. Calculations show that when the length of the constrictions, l, and the length of sidearms, w_4, are greater than the half width of the constrictions, $w_2/2$, (the

above parameters are defined in figure 1), the positions of both resonance levels E_r and E_r' depend neither on the length of the side arms nor on the length of the constrictions. Under this condition they reach their asymptotic values corresponding to the case of intersection of two infinite perpendicular quantum wires [4]: $E_r \simeq 0.66E_1^{th}$ and $E_r' \simeq 0.93E_2^{th}$, where $E_1^{th} = \hbar^2/(2m^*)(\pi/w_2)^2$ and $E_2^{th} = \hbar^2/(2m^*)(2\pi/w_2)^2$ are the propagation threshold energy for the first and the second mode correspondingly. The width Γ of the first resonance is also independent of w_4 if $w_4 \geqslant w_2/2$ and is determined, besides the threshold energy, $E_{th} \equiv E_1^{th}$, by the length of the narrow constriction. The dependence of Γ/E_{th} on l exhibits an exponential behaviour, see figure 5. This is in a direct analogy with the tunnelling escape rate of electrons from a well of a DBRT structure which depends exponentially on the barrier width, but is insensitive to the width of the well [27].

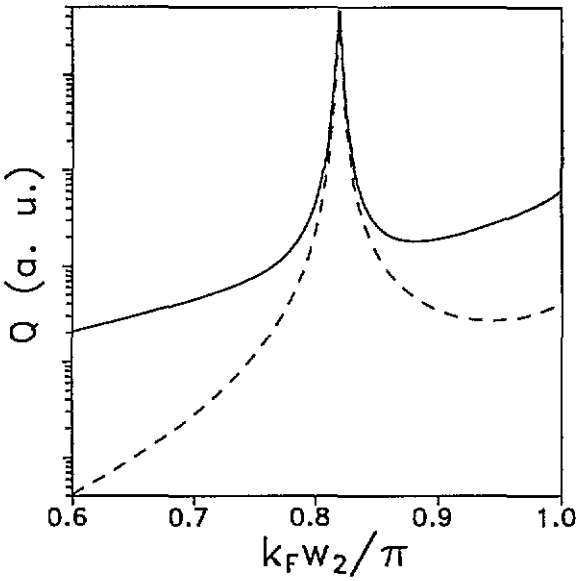

Figure 3. Total charge stored inside the structure (dashed line) and the charge stored in the cavity (region 3, figure 1) (solid line); $l = w_3 = w_4 = w_2$, $w_1/w_2 = 3$.

To conclude this section let us stress that all the presented results refer to an idealized model of a waveguide with abrupt corners and hard-wall confinement. In real structures a split gate defines a rather smooth saddle-shaped potential for the 2DEG [28]. Our calculations for QWRSs with smoothed corners performed on the basis of the recursive Green function technique [29] show that accounting for a more realistic potential can only correct the obtained values of the resonance width and the position of a resonant level, and will not influence the qualitative conclusions about the dependences of E_r and Γ on the parameters of the structure.

4. Bistability behavior of the I–V_g (current–gate voltage) characteristic of the RQWS

In this section we shall apply the results obtained in the previous sections to study resonant transmission through an RQWS of realistic dimensions with charging effects taken into

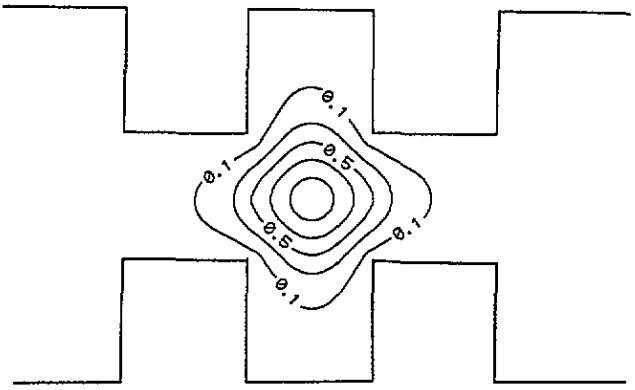

Figure 4. Contour plot of the normalized probability density $\psi\psi^*$ inside the structure at resonance ($k_F w_2/\pi \simeq 0.82$); $l = w_3 = w_4 = w_2$, $w_1/w_2 = 3$.

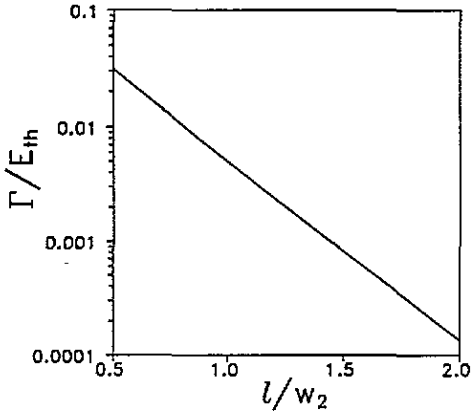

Figure 5. Dependence of the width of the resonance on the length of the constrictions; $w_4 = w_3 = w_2$, $w_1/w_2 = 3$.

account. These effects, as was shown in section 2, are described by the non-linear equation (2), which links the current flowing through the device and the position of the resonant level. In lateral structures, in contrast to the conventional vertical DBRT structures, the position of the resonant level can be easily controlled by the gate voltage V_g. A decrease of V_g enlarges the width of the constrictions w_2^0 and the width of the cavity by the amount $2\Delta w$ and, at the same time, reduces the length of the constrictions l^0 (the length of the side arms w_4^0 remains unchanged), see figure 1. Thus, the dependence of the conductance $G = I/V$ on the width $w_2 = w_2^0 + 2\Delta w$ (at fixed bias V) corresponds to the I–V_g characteristic of the RQWS. In the linear regime of electron transport, when charging effects are disregarded, this dependence is presented in figure 2.

In the following analysis of equation (6) let us suppose that the capacitance C is the self-capacitance between the cavity and infinity. Assuming for simplicity that charge is

concentrated in a sphere of radius $R = w_2$ (see figure 4), one has $C = 4\pi\epsilon\epsilon_0 w_2$†. This is a lower estimation which does not account for induction of charges in the metal gates and in the n-doped layers of GaAs. Thus, the real capacity is higher than estimated one. The value w_2 in the definition of the capacity is, therefore, a phenomenological parameter of the theory which has to be determined from comparison with experiment. The above estimate, nevertheless, appears to be correct up to a factor of the order of unity [19].

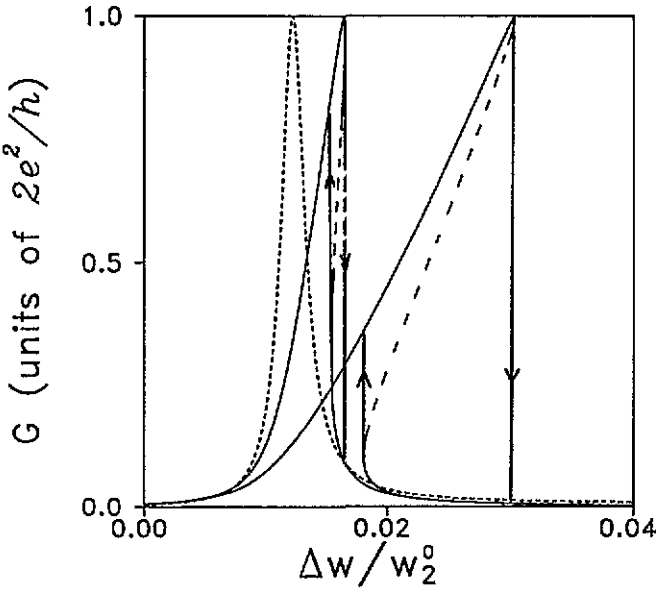

Figure 6. Conductance G as a function of the width of the constrictions w_2 ($w_2 = w_2^0 + 2\Delta w$) calculated on the basis of equation (6). Dashed line corresponds to the linear regime, when no charging effects are taken into account; $k_F w_2^0/\pi = 0.8$, $l^0 = w_3^0 = w_4^0 = w_2^0$, $w_1^0/w_2^0 = 3$. For $w_2^0 = 14$ nm solid lines correspond to (left to right) $V = 0.01$ mV, 0.05 mV.

In our calculations we choose parameters appropriate for a GaAs structure with 2D electron density $n_s = 5 \times 10^{15}$ m^{-2}, $w_2^0 = w_3^0 = w_4^0 = l^0 = 14$ nm, effective mass $m^* = 0.067m_e$ and dielectric constant $\epsilon = 13$. This gives us the threshold energy $E_{th} = 28$ meV, the energy of the quasibound state $E_r = 19$ meV and capacitance $C = 2 \times 10^{-16}$ F. On the basis of the approach of section 3 we have studied the effect of the sample geometry on the resonance width and found that $\Gamma/E_{th} = 0.005\exp(14.6\Delta w/w_2^0)$ (or, $\Gamma = 0.14\exp(14.6\Delta w/w_2^0)$ meV). Using this in equation (6) we obtain the resonance current–gate voltage characteristic of the RQWS, as shown in figure 6. The dotted lines in figure 6 correspond to the physically unrealizible solutions of equation (6), thus the I–V_g characteristic exhibits a hysteresis behaviour. For the given geometry and fixed carrier density, the only parameter in equation (7) which determines the condition for the bistability to occur is the bias voltage V. For the structure under consideration this condition is $V \gtrsim 0.01$ mV. In accordance with equation (9), the greater the bias voltage, the greater the range of bistability. Varying the applied bias influences only the range

† In [19,21] where the radius of the dot r_{dot} was much greater than the width of the 2DEG in the direction of confinement, the capacitance of the device was estimated as the self-capacitance of a disc of radius r_{dot}, $C_{dot} = 8\epsilon\epsilon_0 r_{dot}$.

of bistability and not the maximum current. The latter, for the symmetric structure, is always $I_{max} = 2e^2/h$. These results apply at zero temperature. For higher temperatures, the resonance thermally broadens (Γ increases); therefore, the parameter α in equation (6) decreases and the bistability region is reduced.

Due to the proximity of the continuous spectrum (i.e. $k_F w_2/\pi > 1$) to the quasibound level E_r^0, the Lorentzian approximation (2) is justified only for a limited region of k_F. This limits the use of equation (6) for the description of charging effects in RQWSs: the range of bistability must lie within the range where the Lorentzian approximation (2) is justified. For example, for the structure under consideration, the approximation (2) is valid when the current drop does not exceeds two orders of magnitude, see figure 7.

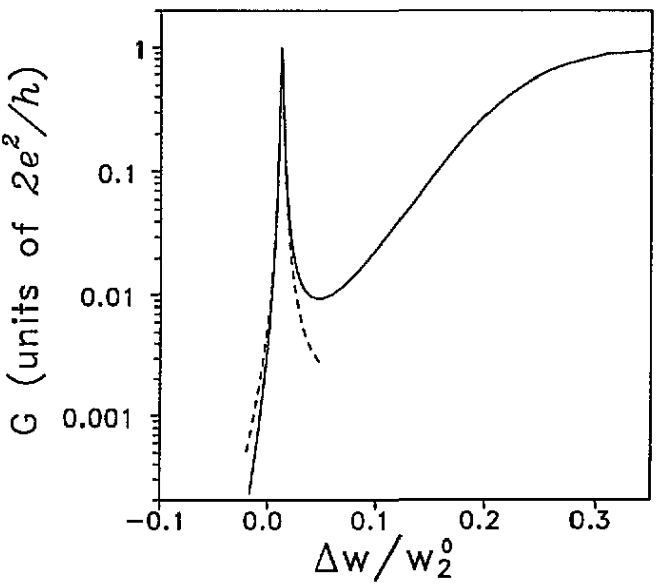

Figure 7. Conductance G as a function of the width of the constrictions w_2 ($w_2 = w_2^0 + 2\Delta w$) calculated on the basis of (10)–(13) (no charging effects are taken into account). Dashed line is the Lorentzian approximation, equation (2); $l^0 = w_3^0 = w_4^0 = w_2^0$, $w_1^0/w_2^0 = 3$.

In our model we also neglected the contribution to the current from the electrons tunnelling through the depletion regions underneath the gates. This is justified for the case when the gate voltage is high enough and w_1 is not much greater and l is not much smaller than the width of the constriction w_2.

To conclude, let us stress that in RQWSs changing the resonant level by varying the gate voltage does not destroy the symmetry of the device, thus full transmission, $T = 1$, can be achieved at resonance. On the other hand, in vertical DBRT structures, effective control of the resonant level can be realized only by varying the applied bias. But changing the bias inevitably introduces asymmetry in the structure. This drastically reduces the total transmission [30]. Therefore, to enhance the resonance and to enlarge the range of bistability it is necessary to have highly asymmetrical and opaque barriers at zero bias. This has a rather unpleasant consequence: one needs a large bias ($\sim$ 100 mV–1 V) to reach resonance in realistic samples. In this case the influence of the absorption and depletion regions in the formation of a potential throughout the device cannot be neglected. This effect, as well as effects of the biasing circuit, are usually not taken into account in the

model Hamiltonian. As a result, the comparison of experimental data with theoretical predictions is rather ambiguous. In contrast, in experiments on the conductivity of 2D lateral structures, the small bias voltages ($\sim$ 10 mV or less) used produce only small corrections to the equilibrium distribution in the emitter and collector regions. Therefore, effects of the accumulation and depletion layers on the electron transmission through the device are not as important as in the case of the DBRT structures. This allows one to distinguish more clearly the origin of the bistability, and to remove the existing uncertainty in the interpretation of experimental data.

5. Brief summary

In summary, effects of the space–charge formation in electron transport in RQWS and its manifestation in the current–gate voltage characteristic of the device have been investigated. The change of the potential profile inside the structure, due to the excess charge stored in the dot when the resonant condition holds, is explicitly taken into account. The value of the conduction band shift is assumed to be determined by the gain in electrostatic energy associated with the charging of the cavity. A closed non-linear equation relating the resonant current flowing through the RQWS to the energy of the resonant level (which can be varied by changing the applied gate voltage) is derived for the case of the linear-response regime. It is shown that the current–gate voltage characteristic of the RQWS exhibits a bistable behaviour if the maximum shift of the conduction band in the cavity caused by the excess charge exceeds roughly the width of the resonance. The energy region where bistability occurs is proportional to the applied bias and inversely proportional to the half width of the resonance. The latter is calculated within the framework of a standard match-mode technique using an idealized model of a waveguide with hard-wall confinement and abrupt constrictions. The dependence of the resonant width on the device geometry is investigated and, on the basis of the above results, the bistability in the I–V_g characteristic (current–gate voltage) is studied for structures of realistic dimensions.

Acknowledgments

I am grateful to Professor E H Hauge for discussions of this work and critical reading of the manuscript. I have also benefited from discussions with Professor K A Chao on bistability phenomena in resonant tunnelling structures. Especially I deeply appreciate extensive interaction with Professor A I Onipko during all stages of this work. I am pleased to acknowledge the support of the Royal Norwegian Council for Scientific and Industrial Research (NTNF).

References

[1] Beenakker C W J and van Houten H 1991 *Solid State Physics, Advances in Research and Applications* vol 44, ed H Ehrenreich and D Turnbull D (San Diego: Academic)

[2] Kouwenhoven L 1992 *Physics of Low-Dimensional Semiconductor Structures* ed P N Bucher *et al* (New York: Plenum)

[3] Wharam D A, Thornton T J, Newbury R, Pepper M, Ahmed H, Frost J E F, Hasko D G, Peacock D C, Ritchie D A and Jones G A C 1988 *J. Phys. C: Solid State Phys.* 21 L209
van Wees B J, van Houten H, Beenakker C W J, Williamson J G, Kouwenhoven L P, van der Marel D and Foxon C T 1988 *Phys. Rev. Lett.* 60 848

Szafer A and Stone A D 1989 *Phys. Rev. Lett.* **62** 300
Haanapel E G and van der Marel D 1989 *Phys. Rev.* B **39** 5489
Kirczenov G 1989 *Phys. Rev.* B **39** 10452
[4] Schult R L, Ravenhall D G and Wyld H W 1989 *Phys. Rev.* B **39** 5476
Peeters F M 1989 *Supperlatt. Microstruct.* **6** 217
[5] Weisshaar A, Lary J, Goodnick S M and Tripathi V K 1991 *IEEE Electron Devices Lett.* **12** 2
[6] Weisshaar A, Lary J, Goodnick S M and Tripathi V K 1991 *J. Appl. Phys.* **70** 355
[7] Takagaki Y and Ferry D K 1992 *Phys. Rev.* B **45** 13,494
[8] Berggren K F and Zhen-Li Ji 1991 *Phys. Rev.* B **43** 4760
Berggren K F, Besev C and Zhen-Li Ji 1992 *Phys. Scr.* T **42** 141
[9] Davydov A S and Ermakov V N 1987 *Physica* **28D** 168
[10] Sheard F W and Toombs G A 1988 *Appl. Phys. Lett.* **52** 1228
[11] Bandara K M S V and Coon D D 1988 *Appl. Phys. Lett.* **53** 1865
[12] Kluksdahl N, Kriman A M, Ferry D K and Ringhofer C 1989 *Phys. Rev.* B **39** 7720
[13] Mains R K, Sun J P and Haddad G I 1989 *Appl. Phys. Lett.* **55** 371
[14] Rahman M and Davies H J 1990 *Semicond. Sci. Technol.* **5** 168
[15] Malysheva L I and Onipko A I 1992 *Phys. Rev.* B **46** 3906
[16] Zou N, Willander M, Linnerud I, Hanke U, Chao K A and Galperin Yu M 1994 *Phys. Rev.* **49** 2193
[17] Goldman V J, Tsui D C and Cunningham J E 1987 *Phys. Rev. Lett.* **58** 1257; 1987 *Phys. Rev. Lett.* **59** 1623
Zaslavsky A, Goldman V J, Tsui D C and Cunningham J E 1988 *Appl. Phys. Lett.* **53** 1408
Alves E S, Eaves L, Henini M, Hughes O H, Leadbeater M L, Sheard F W, Toombs G A, Hill G and Pate M A 1988 *Electron. Lett.* **24** 1190
Leadbeater M L, Alves E S, Eaves L, Henini M, Huges O H, Sheard F W and Toombs G A 1988 *Semicond. Sci. Technol.* **3** 1060
[18] Scott-Thomas J H F, Field S B, Kastner M.A, Smith H I and Antoniadis D A 1989 *Phys. Rev. Lett.* **62** 583
Field S B, Kastner M A, Meirav U, Scott-Thomas J H F, Antoniadis D A, Smith H I and Wind S J 1990 *Phys. Rev.* B **42** 3523
Meirav U, Kastner M A and Wind S J 1990 *Phys. Rev. Lett.* **65** 771
[19] Kouwenhoven L P, van der Vaart N C, Johnson A T, Kool W, Harmans C J P M, Williamson J G, Staring A A M and Foxon C T 1991 *Z. Phys.* B **85** 367
[20] van Houten H and Benakker C W J 1989 *Phys. Rev. Lett.* **63** 1893
Glazman L I and Shekhter R I 1989 *J. Phys.: Condens. Matter* **1** 5811
Groshev A, Ivanov T and Valtchinov V 1991 *Phys. Rev. Lett.* **66** 1082
[21] Averin D V, Korotkov N N and Likharev K K 1991 *Phys. Rev.* B **44** 6199
[22] See for a review Averin D V and Likharev K K 1990 *Quantum Effects in Small Disordered Systems* ed B Al'tshuler *et al* (Amsterdam: Elsevier)
[23] Landauer R 1981 *Phys. Lett.* **85A** 91
Fisher D S and Lee P A 1981 *Phys. Rev.* **23** 6851
Landauer R 1989 *J. Phys.: Condens. Matter* **1** 8099
[24] Landau L D and Lifshitz I M 1974 *Quantum Mechanics* (Moscow: Nauka) (in Russian)
Stone A D and Lee P A 1985 *Phys. Rev. Lett.* **54** 1196
Price P J 1988 *Phys. Rev.* B **38** 1994
[25] Bagwell P F and Orlando T P 1989 *Phys. Rev.* B **40** 1456
[26] Gaididei Yu B, Malysheva L I and Onipko A I 1992 *J. Phys.: Condens. Matter* **4** 7103
Klimenko Yu A, Malysheva L I and Onipko A I 1992 *J. Phys.: Condens. Matter* **5** 5215
Onipko A I and Zozulenko I V 1993 *Semicond. Sci. Technol.* **8** 2115
[27] Zou N, Rammer J and Chao K A 1992 *Phys. Rev.* B **46** 15912
[28] Kumar A, Laux S E and Stern F 1990 *Phys. Rev.* B **42** 5166
[29] Fisher D S and Lee P A 1981 *Phys. Rev.* B **23** 6851
[30] Ricco B and Azbel M 1984 *Phys. Rev.* B **29** 1970